International Journal of Nanomedicine

Dovepress
open access to scientific and medical research

Open Access Full Text Article

ORIGINAL RESEARCH

Promoting tendon to bone integration using graphene oxide-doped electrospun poly(lactic-co-glycolic acid) nanofibrous membrane

This article was published in the following Dove Medical Press journal:
International Journal of Nanomedicine

Wei Su[1]
Zhiying Wang[2]
Jia Jiang[1]
Xiaoyun Liu[2]
Jinzhong Zhao[1]
Zhijun Zhang[2]

[1]Department of Sports Medicine, Shanghai Jiao Tong University Affiliated Sixth People's Hospital, Shanghai, China; [2]Suzhou Key Laboratory of Nano-Bio Interface, Division of Nanobiomedicine, Suzhou Institute of Nano-Tech and Nano-Bionics, Chinese Academy of Sciences, Suzhou, Jiang Su, China

Background: These normal entheses are not reestablished after repair despite significant advances in surgical techniques. There is a significant need to develop integrative biomaterials, facilitating functional tendon-to-bone integration.

Materials and methods: We fabricated a highly interconnective graphene oxide-doped electrospun poly(lactide-co-glycolide acid) (GO-PLGA) nanofibrous membrane by electrospinning technique and evaluated them using in vitro cell assays. Then, we established rabbit models, the PLGA and GO-PLGA nanofibrous membranes were used to augment the rotator cuff repairs. The animals were killed postoperatively, which was followed by micro-computed tomography, histological and biomechanical evaluation.

Results: GO was easily mixed into PLGA filament without changing the three dimensional microstructure. An in vitro evaluation demonstrated that the PLGA membranes incorporated with GO accelerated the proliferation of BMSCs and furthered the Osteogenic differentiation of BMSCs. In addition, an in vivo assessment further revealed that the local application of GO-PLGA membrane to the gap between the tendon and the bone in a rabbit model promoted the healing enthesis, increased new bone and cartilage generation, and improved collagen arrangement and biomechanical properties in comparison with repair with PLGA only.

Conclusion: The electrospun GO-PLGA fibrous membrane provides an effective approach for the regeneration of tendon to bone enthesis.

Keywords: enthesis, osteogenic material, cartilage, collagen arrangement, rabbit model

Introduction

The enthesis is a special complex tissue interface that connects mechanically dissimilar tissues and transfers stress between tendon/ligament and bone.[1,2] Several common sports medicine injuries, including rotator cuff tendon tear and cruciate ligament rupture, require the reconnection of tendon or ligament to bone.[3,4] Promoting the healing of the bone and tendon/ligament at the implant site is particularly important clinically.[5] However, these normal critical entheses are not reestablished after repair despite significant advances in surgical techniques.[6,7] In fact, the new connections of tendon or ligament to bone are filled with the mechanically inferior fibrovascular scar tissue, which compromises the long-term clinical outcome. For this reason, there is a significant need to develop integrative biomaterials, facilitating functional tendon to bone integration.

Recently, some studies put emphasis on electrospun fibrous membranes for tissue regeneration and loading growth factors because of their high porosity.[8,9] Lots of biomaterials are fabricated into scaffolds or membranes with different sized fibers by the electrospinning technique, and the diameter of the nanofibers is similar to type I collagen.[5] The three-dimensional porous structure of fibrous membranes mimics the natural structure

Correspondence: Jinzhong Zhao
Department of Sports Medicine, Shanghai Jiao Tong University Affiliated Sixth People's Hospital, 600 Yishan Road, Shanghai 200233, China
Tel +86 21 6436 9181
Email zhaojinzhongdoctor@163.com

Zhijun Zhang
Suzhou Key Laboratory of Nano-Bio Interface, Division of Nanobiomedicine, Suzhou Institute of Nano-Tech and Nano-Bionics, Chinese Academy of Sciences, 398 Ruoshui Road, Suzhou 215123, Jiang Su, China
Tel +86 512 6348 1450
Email zjzhang2007@sinano.ac.cn

submit your manuscript | www.dovepress.com
Dovepress
http://dx.doi.org/10.2147/IJN.S183842

net and is the ideal substrate for tissue cell attachment and proliferation.[10] Synthetic poly(lactic-co-glycolic acid) (PLGA) has been widely used in forming an electrospun fibrous membrane with proper mechanical properties and low immunogenicity and toxicity.[11,12] Furthermore, it can be structured to degrade when the tissue grows into its structure.[13] However, PLGA lacks an excellent osteoinductivity ability, which restricts its independent application in the field of orthopedics.

Graphene oxide (GO), one of the most important derivatives of graphene, is a two-dimensional carbon material with many impressive properties, including sp^2 carbon domains, large surface area, and hydrophilic groups, and it has received much focus in the area of biomedical engineering.[14,15] Previous research demonstrated that GO bound aromatic anticancer drugs and proteins through electrostatic interaction, π–π stacking, and hydrophobic interaction.[16,17] Previous studies have also shown that mesenchymal stem cells proliferated quickly and could differentiate into osteoblasts under the induction of GO.[18,19] It is known that bone marrow mesenchymal stem cells (BMSCs) migrate to the bone tunnels after cruciate ligament reconstruction or to the cancellous bone surface after tendon footprint preparation and differentiate into osteoblasts.[20,21] Previous research showed that the development process of the tendon to bone enthesis was similar to the process of endochondral bone formation.[22] The osteogenic ability of biomaterial scaffolds is critical for enhancing tendon/ligament to bone integration. It is reported that the osteoconductive calcium phosphate materials had positive effects on tendon to bone healing in vivo.[23,24] Accordingly, we speculate that GO enhances the osteointegration of tendon/ligament to bone, utilizing its osteogenic characteristics. To exhibit its ideal effects, GO needs to be combined with scaffolds to distribute uniformly in the tendon/ligament to bone interface. In addition, retaining the GO at the injured part of the body for a persistent period is necessary, which keeps the desired effect and reduces the potentiality of heterotopic ossification.[25] With the electrospinning technique, GO is dispersed in the PLGA nanofibrous membrane and avoids being transferred to the surrounding tissues.

The aim of this study was to comprehensively investigate the effect of the GO-PLGA nanofibrous membrane on osteointegration in a rabbit supraspinatus tendon repair model (Figure 1). To prove our hypothesis, highly interconnective PLGA/GO-PLGA fibrous membranes were fabricated and characterized, and their effects on the proliferation and differentiation of BMSCs in the rabbit were investigated. Then, the PLGA/GO-PLGA fibrous membranes were used to investigate the effect on tendon to bone integration in a rabbit model.

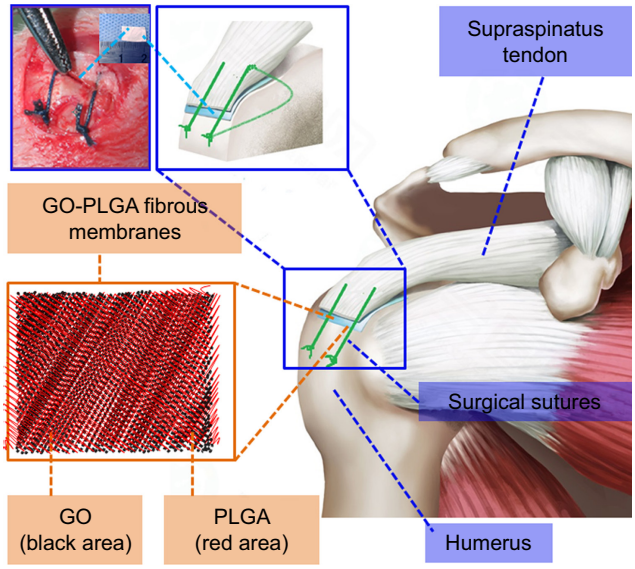

Figure 1 Diagram of transosseous supraspinatus tendon repair with GO-PLGA fibrous membranes.
Abbreviations: GO, graphene oxide; PLGA, poly(lactic-co-glycolic acid).

Materials and methods

Fabrication of the GO-PLGA nanofibrous membranes

A 15 wt% PLGA suspension was mixed with 1% GO. Briefly, 30 mg GO was dispersed in a 20 mL mixed solvent of tetrahydrofuran and dimethylformamide (3/1, v/v) for 24 h with a magnetic stirrer at 4°C, and 3 g of PLGA was mixed into the solvent. An ultrasonic wave cleaner (50 W, SK1200H; Shanghai KUDOS, Shanghai, China) was used to sonicate this solution for 10 min. The PLGA/GO suspension was put into a syringe with a needle. The equipment supply (BGG40/2; Institute of Beijing High Voltage Technology, Beijing, China) was linked with the needle. An aluminum board served as the ground collector. The distance between the pinpoint and collector was 20 cm, and the applied voltage was 10 kV. The nanofibrous membranes were dried to remove the trace solvent at 37°C and were kept in a dryer at 4°C for further use.

Characterization of the nanofibrous membranes

The net structure of the nanofibrous membranes was scanned by scanning electron microscopy (S-4800; Hitachi Ltd., Tokyo, Japan), according to the procedures described by a previous study.[26] The mechanical characters of the PLGA and GO-PLGA membranes were measured by a mechanical test device (H5K-S; Hounsfield, Salfords, UK). The stress–strain curve of these membranes was obtained from the deformation curves at a tensile speed (0.5 mm/s).

Proliferation and osteogenic differentiation of rabbit BMSCs

Before BMSC seeding, sterilization of the PLGA and GO-PLGA nanofibrous membranes was conducted, followed by washing and soaking overnight in cell medium. A total of 1×10^4 rabbit BMSCs were cultured on these nanofibrous membranes and were placed in a 24-well plate for 1, 3, and 7 days under the condition of 5% CO_2 at 37°C. Rabbit BMSCs cultured in plates without nanofibrous membranes were used as the blank control (BC). The proliferation of the BMSCs was evaluated with a Cell Counting Kit-8 (Dojindo Molecular Technologies, Kumamoto, Japan). The absorbance was recorded at 450 nm by an ELX Ultra Microplate Reader (Bio-tek, Winooski, VT, USA). The osteogenic differentiation of the rabbit BMSCs was evaluated by the ALP activity and alizarin red staining. A total of 1×10^5 rabbit BMSCs were seeded on the PLGA and GO-PLGA nanofibrous membranes in a 24-well plate for 7 and 14 days. Rabbit BMSCs cultured in plates without nanofibrous membranes were also used as the BC. After the coculture, the nanofibrous membranes/cells were treated with cell lysis medium for a whole night at 4°C. The ALP activity was assessed by a test kit (ALP kit; Nanjing Jiancheng Institute of Biotechnology, Nanjing, China) according to the manufacturer's instructions. The absorbance was obtained at 520 nm. With the above-mentioned culturing procedure for rabbit BMSCs, after coculture for 14 days these nanofibrous membranes were washed with PBS three times, and the paraformaldehyde solution was used to fixed membranes for 10 min. The membranes were finally stained with an alizarin red solution for 30 min and washed with PBS three times again. After the alizarin red staining, images of the BC, PLGA, and GO-PLGA nanofibrous membranes groups were captured by microscope (DM4000B; Leica Microsystems, Wetzlar, Germany).

Rabbit supraspinatus tendon repair model

The procedures of animal experiments were in strict accordance with the policy of the Institutional Animal Care and Use Committee of Shanghai Jiao Tong University Affiliated Shanghai Sixth People's Hospital, and the Animal Welfare Ethics Committee of Shanghai Sixth People's Hospital approved this study. A total of 108 mature male rabbits (weight 3.0±0.3 kg) were used. All of the rabbits underwent transosseous supraspinatus tendon repair. Under general anesthesia, one of the shoulders was shaved and then 2.5% iodophors were used to sterilize the incision skin. The insertion of the supraspinatus tendon was exposed and excised through an anterior superolateral approach for the shoulder joint. The native enthesis was decorticated with a No 15 blade knife. Two 1.2-mm-diameter bone tunnels were drilled through the greater tuberosity of the humerus. In the experimental groups, the PLGA and GO-PLGA nanofibrous membranes were interposed between the supraspinatus tendon and humerus bone, and No 2-0 nylon sutures were passed through the tendon, nanofibrous membrane, and bone tunnels and were tied to fix the tendon to the bone (Figure S1). In the control group, the tendon was sutured back to the bone without any nanofibrous membrane interposition. The surgical incision was closed. Postoperatively, the rabbits were allowed to move freely after the operation. All rabbits were sent back to their cages and given 0.05 mg/kg buprenorphine two times a day for 4 days to reduce pain. At 4, 8, and 12 weeks, six supraspinatus tendon–humerus complexes were sacrificed for microcomputed tomography (micro-CT) and histology examination, and six complexes were used for biomechanical testing.

Micro-CT analysis

The newly formed bone and bone density on the greater tubercles were evaluated with a micro-CT machine (eXplore Locus SP; GE Healthcare, London, ON, Canada). Each tendon–humerus complex was scanned at a voltage of 90 kV, 270 mA, and a 0.018-mm effective pixel size. After thresholding, three-dimensional reconstruction images were obtained. A uniform 5×11 mm^2 cylindroid region of interest (ROI) was selected at the surface of the tendon–humerus complex footprint. The ROI included a portion of the connection of the tendon and the humerus bone. The bone mineral density and bone volume fraction (bone volume/total volume [BV/TV]) were calculated over the ROI.

Histological analysis

For the histological observation, the supraspinatus tendon–humerus complexes were fixed, dehydrated, decalcified, and embedded. Five-micrometer serial sections were cut from each paraffin block in the repaired tendon direction. H&E, Safranin O/Fast Green, and picrosirius red stainings were performed and the morphological changes were evaluated. The images of the H&E and Safranin O/Fast Green staining sections were taken by a microscope (DM4000B; Leica Microsystems). The images of the picrosirius red staining sections were captured with a polarized light microscope (Eclipse E800; Nikon Instruments, Melville, NY, USA) for semiquantitatively analyzing the collagen maturation at the connection of the tendon to bone, following the procedure reported in a previous study.[25]

Biomechanical testing

The cross-sectional area of the tendon at the insertion site was measured by a digital caliper after the supraspinatus tendon–humerus complexes were harvested from the rabbits. All of the specimens were frozen at −80°C until biomechanical testing. At the time of testing, the supraspinatus tendon was weaved by polyester sutures, and then the polyester sutures were fixed in a screw grip. The proximal humerus was fixed into the polyvinyl chloride cylinder. The supraspinatus tendon was fixed in the direction of the supraspinatus muscle contraction. To define a standard "zero load," 10 consecutive cycles were conducted from a load of 5 N to a peak load of 50 N. After preconditioning, the ultimate load to failure of the supraspinatus tendon–humerus complexes was recorded at a stretching rate of 0.5 mm/min. The load and displacement curve data were obtained with the machine data system. The ultimate stress and stiffness were calculated.

Statistical analysis

The data were presented as the mean±SD. One-way ANOVA with post hoc testing was used to evaluate three groups. Significance was set at $P<0.05$.

Results

Preparation and characterization of PLGA and GO-PLGA nanofibrous membranes

The PLGA and GO-PLGA nanofibrous membranes were fabricated by the electrospinning technique as described in our previous work.[27] The morphology of the fabricated nanofibrous membranes was observed by scanning electron microscopy (Figure 2A). It was clear that both nanofibrous membranes displayed a three-dimensional network with high porosity, the GO was not observed on the surface of the nanofibers, and the mean diameter of the PLGA was 1,341±245 nm. When the GO was doped into the PLGA fibrous mats, the mean diameter of the GO-PLGA fibers became 1,045±189 nm. The influence of the GO on the mechanical property of PLGA fibrous membrane was then investigated. The tensile strengths of the PLGA and GO-PLGA membranes were 2.37±0.31 MPa and 2.05±0.29 MPa, respectively (Figure 2B). It was clear that the breakdown strength and Young's modulus reduced when 1% GO was added into the PLGA.

In vitro rabbit BMSC tests

Figure 3A shows the proliferation behavior of rabbit BMSCs on the nanofibrous mats with culture time. There was no significant difference between the electrospun nanofibrous membrane groups and the BC group after 1 day of coculture with cells ($P<0.01$), but an obvious difference appeared after 3 days. More importantly, when GO was added into the PLGA fibers, the rate of BMSC proliferation increased significantly compared with the PLGA group. Quantitative analysis for ALP activity revealed that the ALP activity of the rabbit BMSCs cultured on the PLGA/PLGA-GO membrane group, by 7 and 14 days, was higher than that on a BC group, and this increase was higher for the PLGA-GO group (Figure 3B). Similar osteogenic differentiation was also demonstrated by alizarin red S staining. Mineralized nodules were observed when the rabbit BMSCs were cultured on the PLGA and PLGA-GO membrane for 14 days (Figure 3C). More distinct nodules formation were observed in the PLGA-GO membrane than in the PLGA membrane. The results indicated that the BMSCs cultured on the nanofibrous membranes could be better induced into osteoblasts and this differentiation was greater on the PLGA-GO nanofibrous membranes.

In vivo macroscopic observations

No obvious infection was found at the operative region in all rabbit shoulders, and no scar adhesion affected the motion of the shoulder. The repaired supraspinatus tendon was connected to the bone in all rabbits during necropsy. There were no obvious differences in the general appearance of the supraspinatus tendon to the bone complexes among the three groups at the time of sacrifice.

Micro-CT evaluation of the supraspinatus tendon to humerus complexes

At each time point, the micro-CT evaluation revealed that the PLGA and GO-PLGA groups possessed more mineralized tissue compared with the control group, which indicated that the nanofibrous membranes provided support for the newly formed bone between the supraspinatus tendon and bone (Figure 4A). Importantly, significant differences in bone mineral density and BV/TV were always found between the PLGA group and the GO-PLGA group at all time points (Figure 4B). In general, these data demonstrated that the GO-PLGA exhibited significant ability to format new bone at the tendon–bone interface and promoted supraspinatus tendon to bone integration.

Histological examination

Cellularity and host tissue response

In the PLGA and GO-PLGA groups, the residual membranes showed a rapid degradation rate at 4 and 8 weeks after

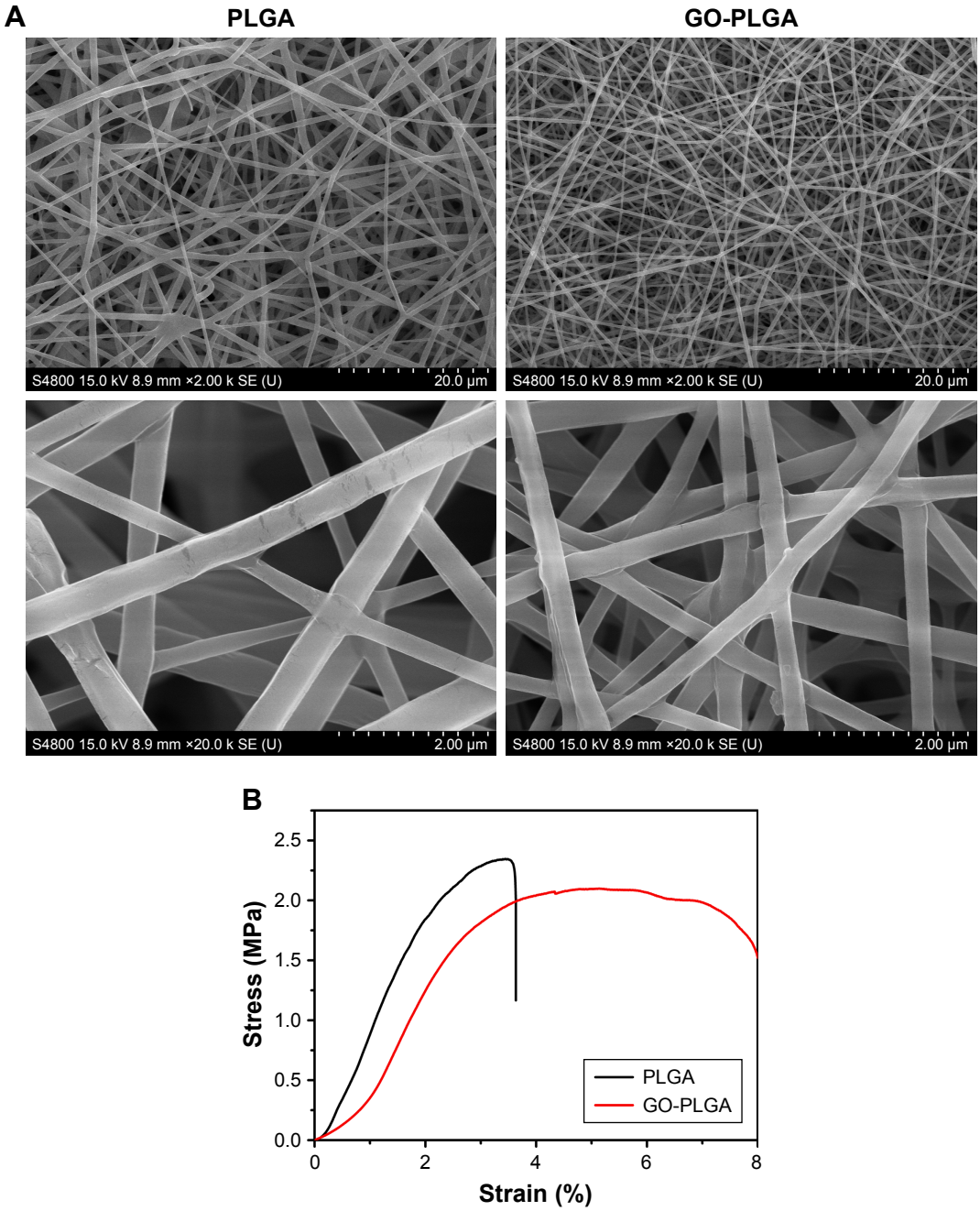

Figure 2 (**A**) Scanning electron microscopy images and (**B**) representative stress–strain curves of electrospun PLGA and GO-PLGA nanofibrous membranes.
Abbreviations: GO, graphene oxide; PLGA, poly(lactic-co-glycolic acid).

operation. At 4 weeks, the membranes began to degrade, and fibroblasts were found in the gap between the fibers and the bundles of the inherent tissue architecture. An irregular arrangement of fibroblasts was observed and microvascules formed at the gap between the GO-PLGA nanofibrous membranes and native tissues. At 8 weeks, the membrane degraded completely. The interfacial tissues began to align regularly and cellularity decreased in the GO-PLGA group from 8 to 12 weeks. In comparison, the fibrovascular granulation tissue of the control group regenerated slowly at each time point (Figure 5).

Metachromasia

The results of the metachromasia staining showed that the interface of the tendon to bone interposed with PLGA and PLGA-GO membranes was entirely connected by a lump of new mineralized tissue (Figure 6). At the time points of 8 and 12 weeks, there was still no new cartilage regeneration in

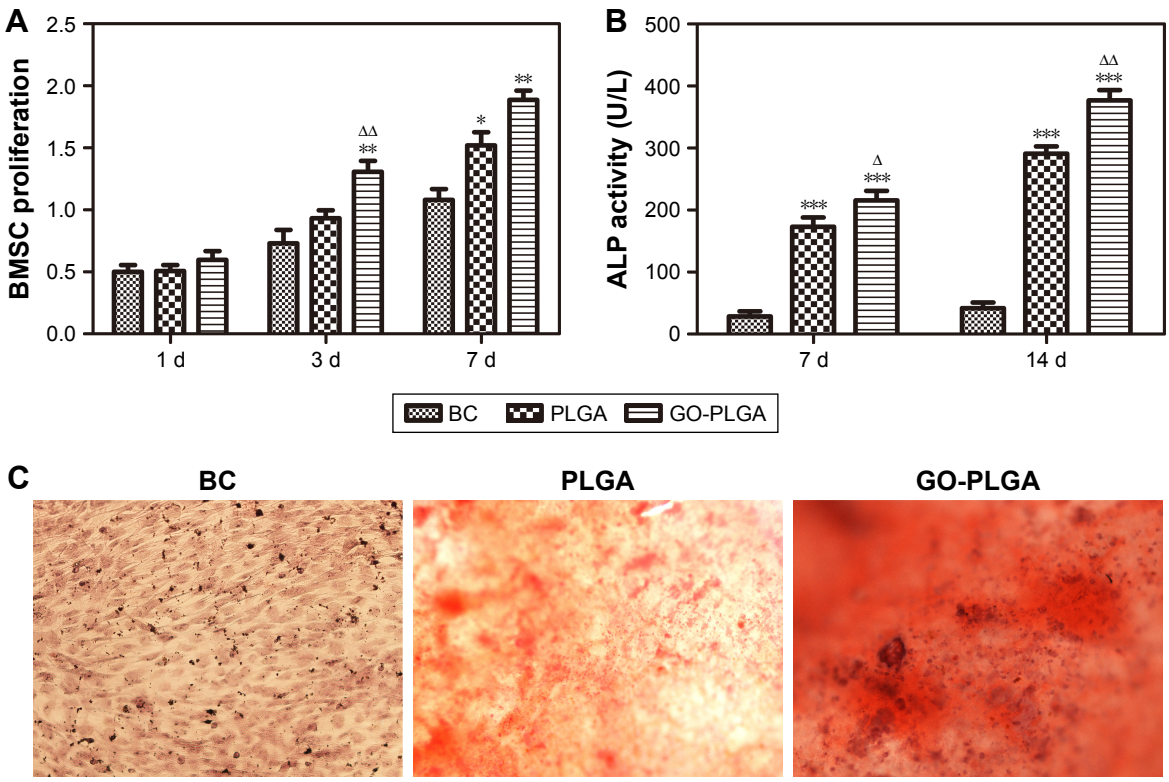

Figure 3 (**A**) CCK-8 assay, (**B**) ALP activity, and (**C**) Alizarin Red staining of the BC, PLGA, and GO-PLGA groups after rabbit BMSCs were seeded onto electrospun nanofibrous membranes.
Notes: Results are presented as the mean±SD (n=3 for each group). *$P<0.05$ vs control; **$P<0.01$ vs control; ***$P<0.001$ vs control; $^{\Delta}P<0.05$ vs PLGA; $^{\Delta\Delta}P<0.01$ vs PLGA.
Abbreviations: BC, blank control; BMSC, bone marrow mesenchymal stem cell; CCK-8, Cell Counting Kit-8; GO, graphene oxide; PLGA, poly(lactic-co-glycolic acid); D, days.

the control group, which was filled with fibrous scar tissue. A few chondrocytes and a certain amount of new bone were found at the interface in the PLGA, while a larger new cartilage formation area was observed in the GO-PLGA group.

Collagen organization

Confirming the initial results of the H&E staining, the picrosirius red-stained sections showed that the collagen fiber bundles of the tendon insertion of the GO-PLGA group aligned more irregularly than the other groups (Figure 7A). At 4 weeks, the tendon insertions of both the control and experimental groups were filled with irregular tissues. At 8 and 16 weeks, the parallel cartilaginous continuity was gradually reestablished along the long axis in the GO-PLGA group. At all time points, the GO-PLGA group exhibited significantly improved type I collagen production at the healing location than the other groups, according to birefringence under polarized light (Figure 7B). There was no significant diversity between the control and PLGA groups at 4 weeks, while the PLGA group exhibited significantly improved type I collagen production at 8 and 12 weeks.

The results of biomechanical testing

At each time point, there was no marked difference in the cross-sectional area of healing connection between the experimental groups and the control group (Figure 8A). The ultimate load to failure, stress, and stiffness of the supraspinatus tendon to humerus complexes were raised in all groups from 4 to 12 weeks (Figure 8B–D). At all time points, the ultimate load and stress value of the supraspinatus tendon to humerus complexes in the GO-PLGA group were significantly higher than those in the control group (Figure 8B and C). The strength of the tendon to humerus complexes in the GO-PLGA group increased more rapidly. However, no significant difference was observed between the control and PLGA groups. The difference in the stiffness of the supraspinatus tendon to humerus complexes between the control and experimental groups began to appear at 12 weeks, and we found no significant difference in stress when comparing the control and PLGA groups (Figure 8D).

Discussion

Over the last decades, tissue engineering has become a potential approach for musculoskeletal tissue regeneration.[28–30]

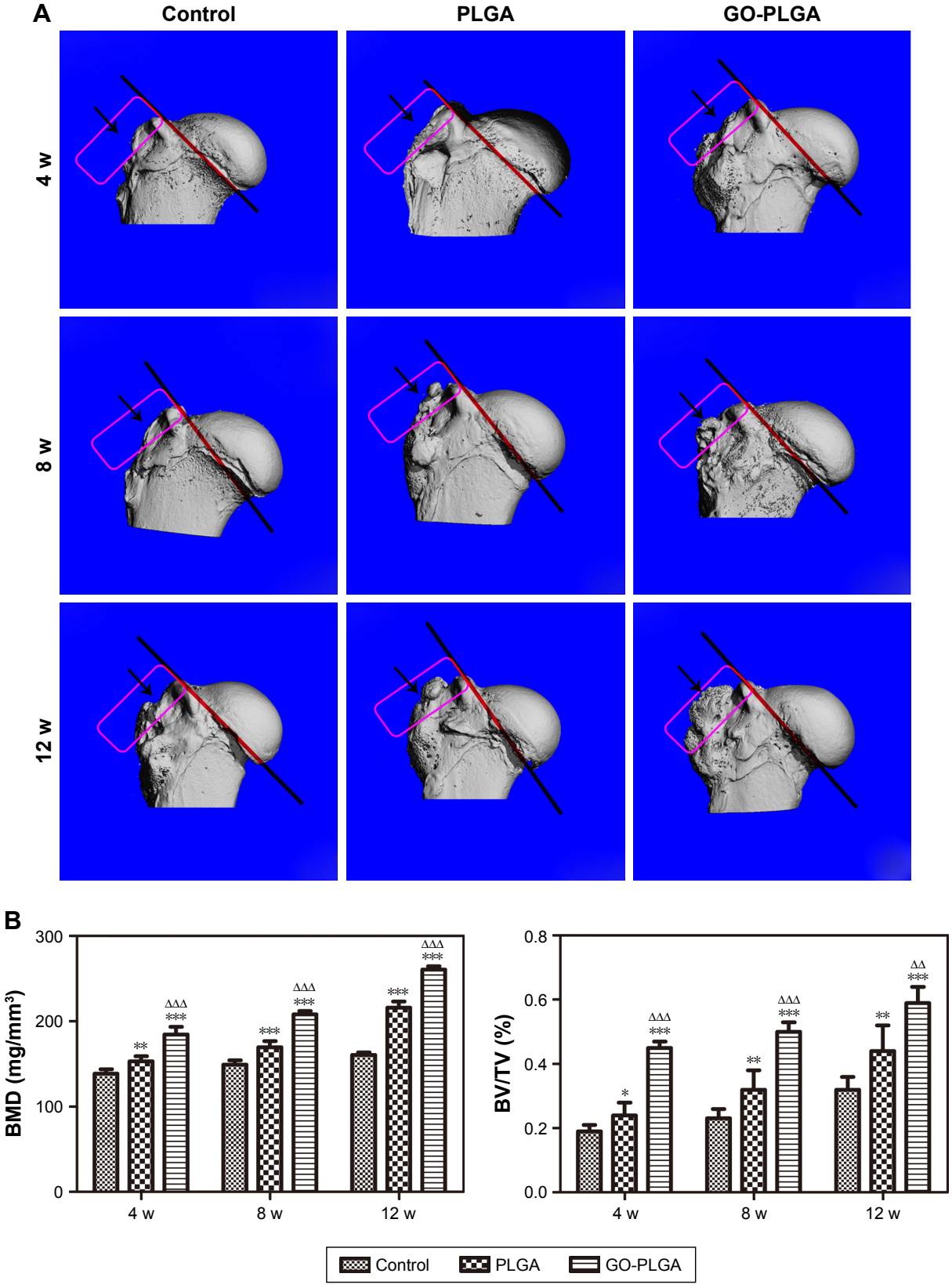

Figure 4 (**A**) Representative microcomputed tomography images of the proximal humerus and (**B**) analysis of BMD and BV/TV.
Notes: Black arrows and red rectangles indicate newly formed bone between supraspinatus tendon and bone. Results are presented as the mean±SD (n=6 for each group). *$P<0.05$ vs control; **$P<0.01$ vs control; ***$P<0.001$ vs control; $^{\Delta\Delta}P<0.01$ vs PLGA; $^{\Delta\Delta\Delta}P<0.001$ vs PLGA.
Abbreviations: BV/TV, bone volume/total volume; BMD, bone mineral density; GO, graphene oxide; PLGA, poly(lactic-co-glycolic acid); W, weeks.

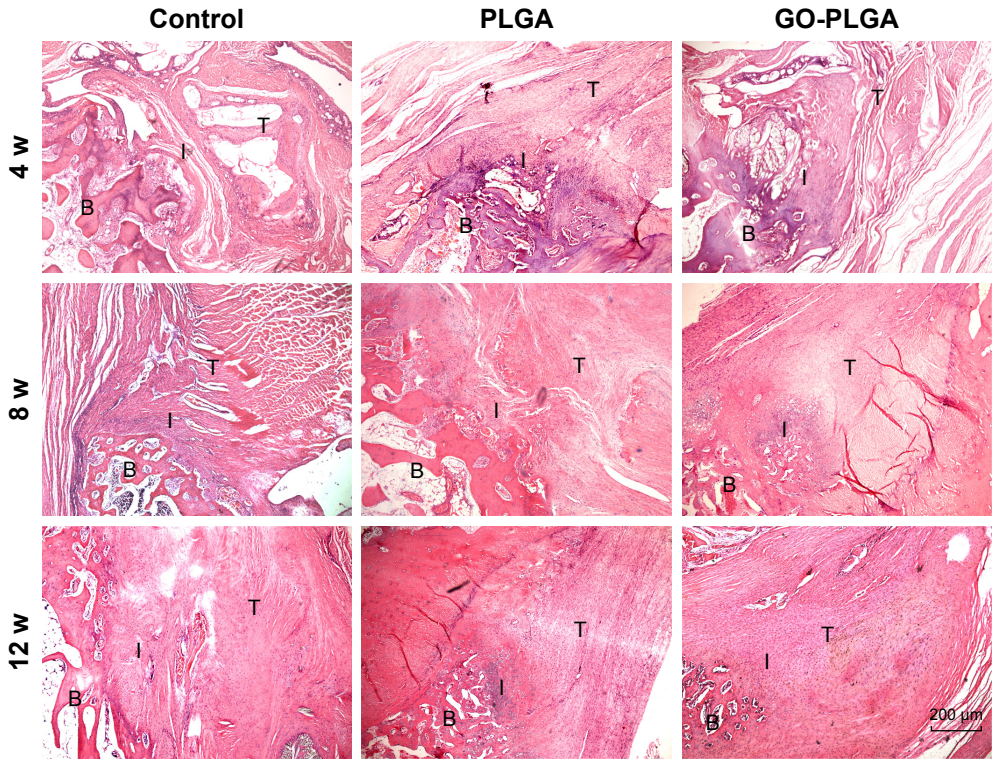

Figure 5 Representative H&E-stained tissue sections (40×) of the supraspinatus tendon insertion site at 4, 8, and 12 weeks postoperatively.
Note: Scale bars for H&E-stained images=200 μm.
Abbreviations: GO, graphene oxide; PLGA, poly(lactic-co-glycolic acid); B, bone; I, interface; T, tendon; W, weeks.

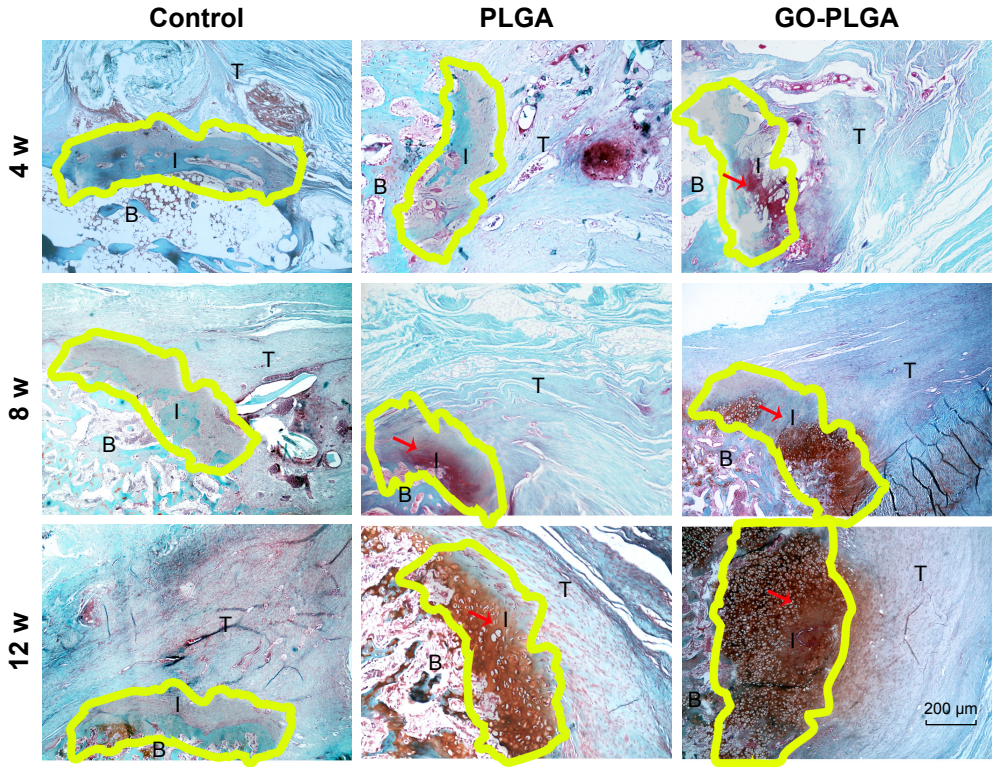

Figure 6 Representative histology images of the cartilage tissue at the insertion site (40× magnification).
Notes: Yellow region indicates newly formed cartilage between supraspinatus tendon and bone. Scale bars for H&E-stained images=200 μm.
Abbreviations: GO, graphene oxide; PLGA, poly(lactic-co-glycolic acid); B, bone; I, interface; T, tendon; W, weeks.

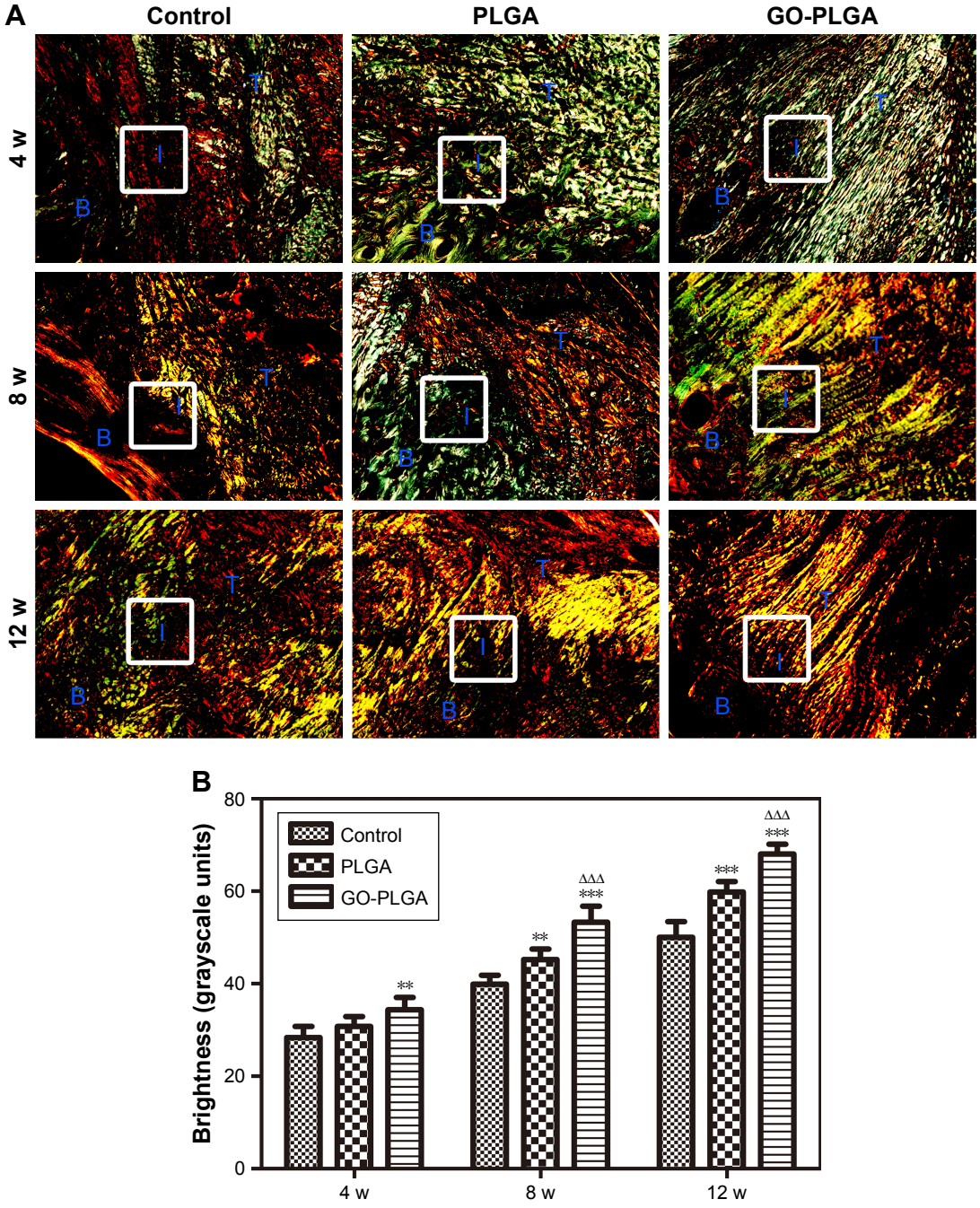

Figure 7 (**A**) Representative picrosirius red-stained tissue sections of the healing enthesis (100×) and (**B**) analysis of the collagen birefringence.
Notes: Rectangle indicates the area of interest for collagen organization. Results are presented as the mean±SD (n=6 for each group). $^{**}P<0.01$ vs control; $^{***}P<0.001$ vs control; $^{\Delta\Delta\Delta}P<0.001$ vs PLGA.
Abbreviations: GO, graphene oxide; PLGA, poly(lactic-co-glycolic acid); B, bone; I, interface; T, tendon; W, weeks.

Tremendous progress has been made in research involving tendon to bone healing using a combination of biomaterials, cells, and growth factors.[6,31–33] In the clinic, the surgically repaired tendon to bone construct is connected by scar formation. The percentage of patients with failure after tendon to bone repair is relatively high.[34–36] The insertion of tendon/ligament and bone is a strong mechanical structure established via a collagen fiber architecture and mineral composition in the native enthesis.[5,37–39] Therefore, it is likely that a fibrous membrane system that generates a fiber architecture and mineral composition will increase the feasibility of tendon to bone healing and may be the key to improve clinical prognosis.

PLGA is considered an excellent biomaterial for bone tissue engineering due to its satisfactory biocompatibility,[40–42]

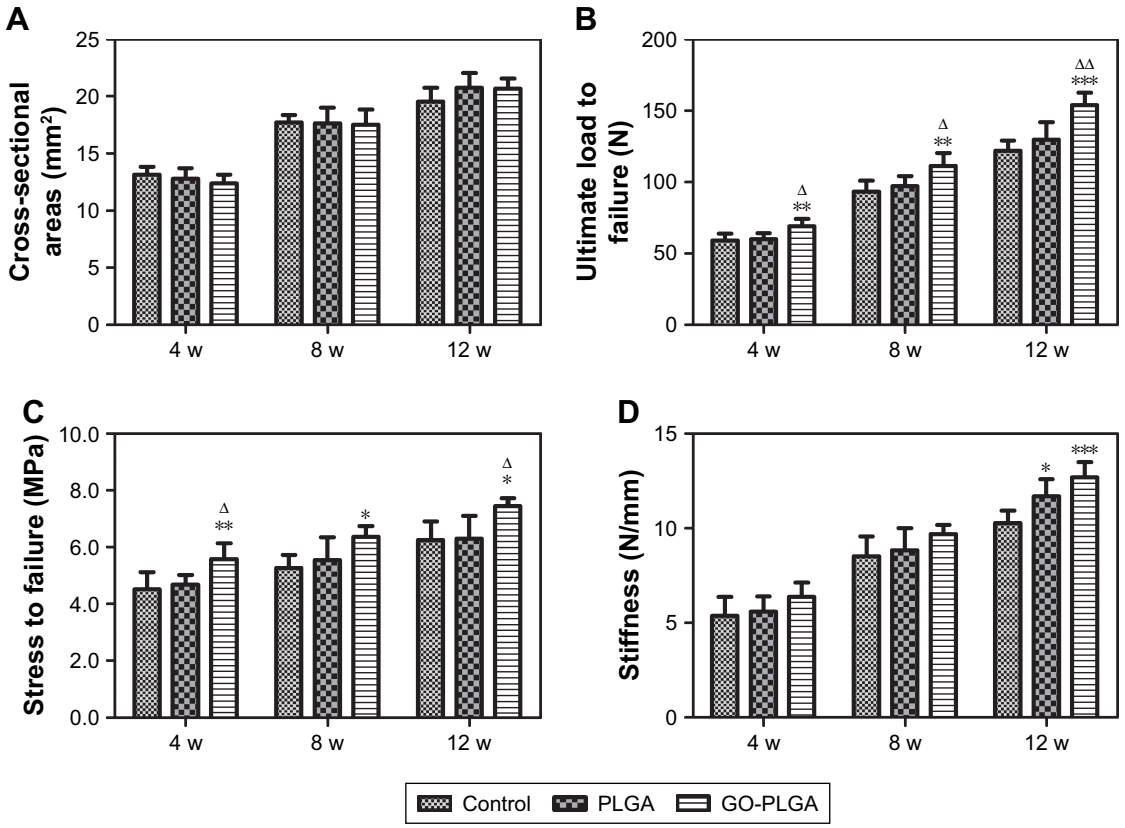

Figure 8 Biomechanical testing of the tendon at the insertion site: (**A**) cross-sectional areas, (**B**) ultimate load to failure, (**C**) stress to failure values, and (**D**) stiffness.
Notes: Results are presented as the mean±SD (n=6 for each group). *$P<0.05$ vs control; **$P<0.01$ vs control; ***$P<0.001$ vs control; $^{\Delta}P<0.05$ vs PLGA; $^{\Delta\Delta}P<0.01$ vs PLGA.
Abbreviations: GO, graphene oxide; PLGA, poly(lactic-co-glycolic acid); W, weeks.

which was also observed in our experiment (Figures 3A and 5). Moreover, the PLGA membrane can be directly placed into the interface of the tendon to bone, conforming to the requirement of local application. Previous research used PLGA to promote tendon to bone healing after rotator cuff repair.[43,44] However, the low osteoinductivity ability of PLGA prevents PLGA from being widely applied in the field of orthopedics, because newly formed bone tissue may be not enough. Similarly, in our study, a few mineralized nodules were observed when cocultured with rabbit BMSCs (Figure 3C), and there was limited newly formed bone tissue in the PLGA group after rotator cuff repair (Figure 4). In order to obtain more new bone formation, and thus tendon healing at the bone interface can be improved, researchers have attempted to use osteo-biomaterials, such as calcium phosphate ceramics and bone morphogenetic proteins.[25,45,46] The in vivo results gained with the osteo-biomaterial were desirable. Previous studies reported that GO exhibits the ability to allow for the migration and growth of osteoblasts and mesenchymal stem cells and had a greater osteoconductivity ability compared with traditional calcium phosphate ceramics.[47–49] Therefore, in this study we fabricated the combined nanofibrous scaffold (GO-PLGA) by the electrospinning technique.

GO has received enormous attention in the bone tissue engineering field due to its unique sp^2 carbon domains, large surface area, and hydrophilic functional group structure.[49–51] The enhanced BMSC growth was probably due to the capability of the adsorption of the protein to the GO-PLGA scaffolds. As shown in Figure 2A, the basic structure of GO-PLGA had a high porosity and surface area, which achieved an appropriate interconnected pore network for new bone formation. Moreover, it was previously reported that GO promotes osteogenesis in vitro.[52–54] Thus, the cell proliferation and ALP activity results demonstrated that PLGA-GO membrane may be conducive to the proliferation and osteogenic differentiation of BMSCs compared with PLGA. The local use of the PLGA-GO membrane in vivo was related to an increase in the area of new cartilage between the tendon and the bone surface. The well-organized collagen fiber orientation at the healing insertion site was consistent with the tensile strength of the tendon, which underlined the significance of GO in the course of tendon–bone healing.

Compared with PLGA, the PLGA-GO investigated in this research was lowly resistant. This can be attributed to its two-dimensional topological plane structure; the GO might be vertical to the nanofibers. When the nanofibers are in a stress state, GO cannot transfer part of the force, resulting in a decrease of the breakdown strength. Although the compression strength of the PLGA-GO fibrous membranes was inferior to the strength of PLGA alone, the biomechanical properties of PLGA-GO are not essential for repairing tendon to bone injury, because the major function of the membranes used between a tendon and bone gap is supporting bone growth rather than bearing mechanical forces.[20] A biomechanical test of the tendon to humerus complex was key to evaluating whether the application of the fibrous membrane improved the biomechanical character of the repaired insertion. In our study, the local implantation of GO-PLGA resulted in a greater ultimate load to failure and stiffness. Furthermore, the mechanical properties of the tendon to humerus complex with GO-PLGA obviously increased after 8 weeks. These results confirmed the practicability of the implantation of GO-PLGA for tendon to bone repair. Although the biomechanical advantages found in this study are comparatively small, they are inspiring and clinically important.

In view of the weaknesses of this study, the implantation of PLGA-GO in patients has a long way to go and further studies are needed. Notably, this study was conducted on a rabbit model rather than the complex condition of a tendon in a human.[55,56] Another limitation of our study is that the last time point we selected is 12 weeks after the operation; it is desirable to carry out histological observation of the tendon to bone junctions even up to 1 year after surgery.[20] Finally, the underlying mechanisms of the promotion of BMSC differentiation and the enhancement of the tendon to bone healing by the nanostructured PLGA-GO membranes are unknown and need to be clarified.

Conclusion

Highly interconnective PLGA/GO-PLGA fibrous membranes were successfully fabricated by the electrospinning technique and were used as a scaffold for tendon to bone healing. GO can be easily mixed into the PLGA filament without changing the three-dimensional microstructure. The GO-doped PLGA nanofibrous mats afford a suitable enthesis microenvironment for BMSC proliferation. An in vitro evaluation demonstrated that the PLGA membranes incorporated with GO accelerated the proliferation of BMSCs and furthered the osteogenic differentiation of BMSCs. In addition, an in vivo assessment further revealed that local application of the GO-PLGA membrane to the gap between the tendon and the bone in a rabbit model promoted the healing enthesis, increased new bone and cartilage generation, and improved collagen arrangement in comparison with repair with PLGA only. These results indicate that the electrospun GO-PLGA fibrous membrane provides an effective approach for the regeneration of tendon to bone enthesis.

Acknowledgment

This work was supported by the National Natural Science Foundation of China (Grant No 81501875 and No 81772341), the CAS "Strategic Priority Research Program" (XDA16020100), and the CAS Key Research Program (ZDRW-ZS-2016-2-4).

Disclosure

The authors report no conflicts of interest in this work.

References

1. Apostolakos J, Durant TJ, Dwyer CR, et al. The enthesis: a review of the tendon-to-bone insertion. *Muscles Ligaments Tendons J*. 2014;4(3):333–342.
2. Benjamin M, Kumai T, Milz S, Boszczyk BM, Boszczyk AA, Ralphs JR. The skeletal attachment of tendons-tendon "entheses". *Comp Biochem Physiol A Mol Integr Physiol*. 2002;133(4):931–945.
3. Peterson JR, Krabak BJ. Anterior cruciate ligament injury: mechanisms of injury and strategies for injury prevention. *Phys Med Rehabil Clin N Am*. 2014;25(4):813–828.
4. Shaffer B, Huttman D. Rotator cuff tears in the throwing athlete. *Sports Med Arthrosc Rev*. 2014;22(2):101–109.
5. Font Tellado S, Balmayor ER, van Griensven M. Strategies to engineer tendon/ligament-to-bone interface: biomaterials, cells and growth factors. *Adv Drug Deliv Rev*. 2015;94:126–140.
6. Atesok K, Fu FH, Wolf MR, et al. Augmentation of tendon-to-bone healing. *J Bone Joint Surg Am*. 2014;96(6):513–521.
7. Lu HH, Thomopoulos S. Functional attachment of soft tissues to bone: development, healing, and tissue engineering. *Annu Rev Biomed Eng*. 2013;15:201–226.
8. Shabafrooz V, Mozafari M, Vashaee D, Tayebi L. Electrospun nanofibers: from filtration membranes to highly specialized tissue engineering scaffolds. *J Nanosci Nanotechnol*. 2014;14(1):522–534.
9. Bhardwaj N, Kundu SC. Electrospinning: a fascinating fiber fabrication technique. *Biotechnol Adv*. 2010;28(3):325–347.
10. Ingavle GC, Leach JK. Advancements in electrospinning of polymeric nanofibrous scaffolds for tissue engineering. *Tissue Eng Part B Rev*. 2014;20(4):277–293.
11. Mundargi RC, Babu VR, Rangaswamy V, Patel P, Aminabhavi TM. Nano/micro technologies for delivering macromolecular therapeutics using poly(D,L-lactide-co-glycolide) and its derivatives. *J Control Release*. 2008;125(3):193–209.
12. Jain RA. The manufacturing techniques of various drug loaded biodegradable poly(lactide-co-glycolide) (PLGA) devices. *Biomaterials*. 2000;21(23):2475–2490.
13. Han FY, Thurecht KJ, Whittaker AK, Smith MT. Bioerodable PLGA-based microparticles for producing sustained-release drug formulations and strategies for improving drug loading. *Front Pharmacol*. 2016;7:185.
14. Chung C, Kim YK, Shin D, Ryoo SR, Hong BH, Min DH. Biomedical applications of graphene and graphene oxide. *Acc Chem Res*. 2013;46(10):2211–2224.

15. Wang Y, Li Z, Wang J, Li J, Lin Y. Graphene and graphene oxide: biofunctionalization and applications in biotechnology. *Trends Biotechnol*. 2011;29(5):205–212.
16. Shen H, Liu M, He H, et al. PEGylated graphene oxide-mediated protein delivery for cell function regulation. *ACS Appl Mater Interfaces*. 2012; 4(11):6317–6323.
17. Kotchey GP, Allen BL, Vedala H, et al. The enzymatic oxidation of graphene oxide. *ACS Nano*. 2011;5(3):2098–2108.
18. Lee WC, Lim CH, Shi H, et al. Origin of enhanced stem cell growth and differentiation on graphene and graphene oxide. *ACS Nano*. 2011;5(9): 7334–7341.
19. Talukdar Y, Rashkow J, Lalwani G, Kanakia S, Sitharaman B. The effects of graphene nanostructures on mesenchymal stem cells. *Biomaterials*. 2014;35(18):4863–4877.
20. Weimin P, Dan L, Yiyong W, Yunyu H, Li Z. Tendon-to-bone healing using an injectable calcium phosphate cement combined with bone xenograft/BMP composite. *Biomaterials*. 2013;34(38):9926–9936.
21. Kida Y, Morihara T, Matsuda KI, et al. Bone marrow-derived cells from the footprint infiltrate into the repaired rotator cuff. *J Shoulder Elbow Surg*. 2013;22(2):197–205.
22. Blitz E, Viukov S, Sharir A, et al. Bone ridge patterning during musculoskeletal assembly is mediated through Scx regulation of BMP4 at the tendon-skeleton junction. *Dev Cell*. 2009;17(6):861–873.
23. Tien YC, Chih TT, Lin JH, Ju CP, Lin SD. Augmentation of tendon-bone healing by the use of calcium-phosphate cement. *J Bone Joint Surg Br*. 2004;86(7):1072–1076.
24. Huangfu X, Zhao J. Tendon-bone healing enhancement using injectable tricalcium phosphate in a dog anterior cruciate ligament reconstruction Model. *Arthroscopy*. 2007;23(5):455–462.
25. Zhao S, Peng L, Xie G, Li D, Zhao J, Ning C. Effect of the interposition of calcium phosphate materials on tendon-bone healing during repair of chronic rotator cuff tear. *Am J Sports Med*. 2014;42(8):1920–1929.
26. Meng J, Han Z, Kong H, et al. Electrospun aligned nanofibrous composite of MWCNT/polyurethane to enhance vascular endothelium cells proliferation and function. *J Biomed Mater Res A*. 2010;95(1):312–320.
27. Luo Y, Shen H, Fang Y, et al. Enhanced proliferation and osteogenic differentiation of mesenchymal stem cells on graphene oxide-incorporated electrospun poly(lactic-co-glycolic acid) nanofibrous mats. *ACS Appl Mater Interfaces*. 2015;7(11):6331–6339.
28. Daly AC, Freeman FE, Gonzalez-Fernandez T, Critchley SE, Nulty J, Kelly DJ. 3D Bioprinting for cartilage and osteochondral tissue engineering. *Adv Healthc Mater*. 2017;6(22):1700298.
29. Padilla S, Sánchez M, Orive G, Anitua E. Human-Based biological and biomimetic autologous therapies for musculoskeletal tissue regeneration. *Trends Biotechnol*. 2017;35(3):192–202.
30. Sankar S, Sharma CS, Rath SN, Ramakrishna S. Electrospun nanofibres to mimic natural hierarchical structure of tissues: application in musculoskeletal regeneration. *J Tissue Eng Regen Med*. 2018;12(1): e604–e619.
31. Lin J, Zhou W, Han S, et al. Cell-material interactions in tendon tissue engineering. *Acta Biomater*. 2018;70:1–11.
32. Patel S, Gualtieri AP, Lu HH, Levine WN. Advances in biologic augmentation for rotator cuff repair. *Ann N Y Acad Sci*. 2016;1383(1):97–114.
33. Nho SJ, Delos D, Yadav H, et al. Biomechanical and biologic augmentation for the treatment of massive rotator cuff tears. *Am J Sports Med*. 2010;38(3):619–629.
34. Weinheimer KT, Smuin DM, Dhawan A. Patient outcomes as a function of shoulder surgeon volume: a systematic review. *Arthroscopy*. 2017; 33(7):1273–1281.
35. Kowalsky MS, Keener JD. Revision arthroscopic rotator cuff repair: repair integrity and clinical outcome: surgical technique. *J Bone Joint Surg Am*. 2011;93(Suppl 1):62–74.
36. Huang R, Wang S, Wang Y, Qin X, Sun Y. Systematic review of all-arthroscopic versus mini-open repair of rotator cuff tears: a meta-analysis. *Sci Rep*. 2016;6:22857.
37. Jensen PT, Lambertsen KL, Frich LH. Assembly, maturation, and degradation of the supraspinatus enthesis. *J Shoulder Elbow Surg*. 2018; 27(4):739–750.
38. Patel S, Caldwell JM, Doty SB, et al. Integrating soft and hard tissues via interface tissue engineering. *J Orthop Res*. 2018;36(4):1069–1077.
39. Zhao S, Su W, Shah V, et al. Biomaterials based strategies for rotator cuff repair. *Colloids Surf B Biointerfaces*. 2017;157:407–416.
40. Martins C, Sousa F, Araújo F, Sarmento B. Functionalizing PLGA and PLGA derivatives for drug delivery and tissue regeneration applications. *Adv Healthc Mater*. 2018;7(1):1701035.
41. Khan I, Gothwal A, Sharma AK, et al. PLGA nanoparticles and their versatile role in anticancer drug delivery. *Crit Rev Ther Drug Carrier Syst*. 2016;33(2):159–193.
42. Mir M, Ahmed N, Rehman AU. Recent applications of PLGA based nanostructures in drug delivery. *Colloids Surf B Biointerfaces*. 2017; 159:217–231.
43. Zhao S, Zhao J, Dong S, et al. Biological augmentation of rotator cuff repair using bFGF-loaded electrospun poly(lactide-co-glycolide) fibrous membranes. *Int J Nanomedicine*. 2014;9:2373–2385.
44. Inui A, Kokubu T, Mifune Y, et al. Regeneration of rotator cuff tear using electrospun poly(d,l-lactide-co-glycolide) scaffolds in a rabbit model. *Arthroscopy*. 2012;28(12):1790–1799.
45. Kovacevic D, Fox AJ, Bedi A, et al. Calcium-phosphate matrix with or without TGF-β3 improves tendon-bone healing after rotator cuff repair. *Am J Sports Med*. 2011;39(4):811–819.
46. Hirakawa Y, Manaka T, Orita K, Ito Y, Ichikawa K, Nakamura H. The accelerated effect of recombinant human bone morphogenetic protein 2 delivered by β-tricalcium phosphate on tendon-to-bone repair process in rabbit models. *J Shoulder Elbow Surg*. 2018;27(5):894–902.
47. Deng W, Qiu J, Wang S, et al. Development of biocompatible and VEGF-targeted paclitaxel nanodrugs on albumin and graphene oxide dual-carrier for photothermal-triggered drug delivery in vitro and in vivo. *Int J Nanomedicine*. 2018;13:439–453.
48. Kenry, Lee WC, Loh KP, Lim CT. When stem cells meet graphene: opportunities and challenges in regenerative medicine. *Biomaterials*. 2018;155:236–250.
49. Shin SR, Li YC, Jang HL, et al. Graphene-based materials for tissue engineering. *Adv Drug Deliv Rev*. 2016;105(Pt B):255–274.
50. Menaa F, Abdelghani A, Menaa B. Graphene nanomaterials as biocompatible and conductive scaffolds for stem cells: impact for tissue engineering and regenerative medicine. *J Tissue Eng Regen Med*. 2015;9(12):1321–1338.
51. Ding X, Liu H, Fan Y. Graphene-based materials in regenerative medicine. *Adv Healthc Mater*. 2015;4(10):1451–1468.
52. Liu H, Cheng J, Chen F, et al. Gelatin functionalized graphene oxide for mineralization of hydroxyapatite: biomimetic and in vitro evaluation. *Nanoscale*. 2014;6(10):5315–5322.
53. Liu X, Shen H, Song S, Chen W, Zhang Z. Accelerated biomineralization of graphene oxide-incorporated cellulose acetate nanofibrous scaffolds for mesenchymal stem cell osteogenesis. *Colloids Surf B Biointerfaces*. 2017;159:251–258.
54. Shao W, He J, Sang F, et al. Enhanced bone formation in electrospun poly(L-lactic-co-glycolic acid)-tussah silk fibroin ultrafine nanofiber scaffolds incorporated with graphene oxide. *Mater Sci Eng C Mater Biol Appl*. 2016;62:823–834.
55. Lebaschi A, Deng XH, Zong J, et al. Animal models for rotator cuff repair. *Ann N Y Acad Sci*. 2016;1383(1):43–57.
56. Deprés-Tremblay G, Chevrier A, Snow M, Hurtig MB, Rodeo S, Buschmann MD. Rotator cuff repair: a review of surgical techniques, animal models, and new technologies under development. *J Shoulder Elbow Surg*. 2016;25(12):2078–2085.

Supplementary material

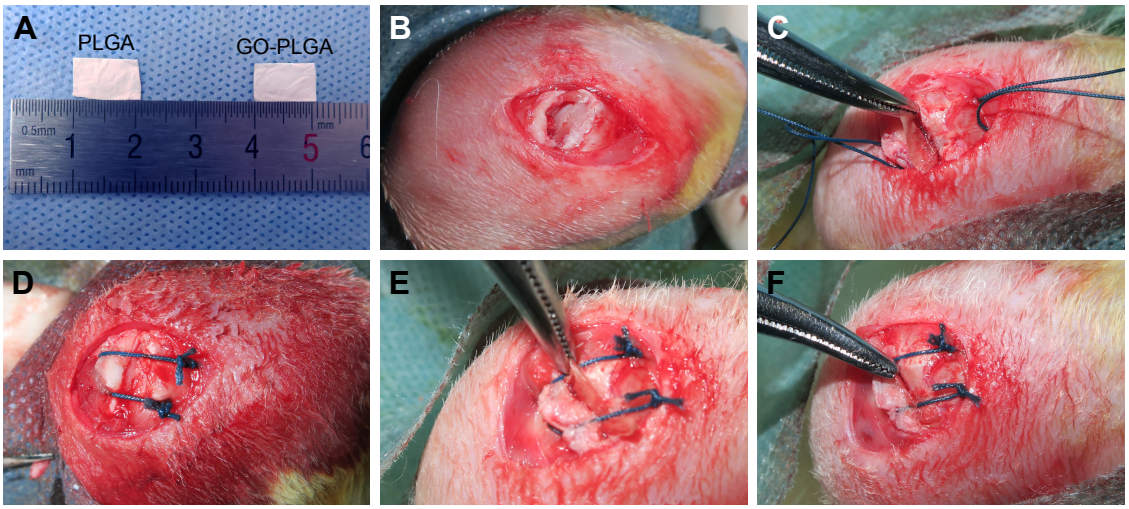

Figure S1 (**A**) General view of PLGA and PLGA-GO membranes and (**B**–**F**) surgical procedure of interposition of PLGA and PLGA-GO membranes in the rabbit supraspinatus tendon repair model.
Abbreviations: GO, graphene oxide; PLGA, poly(lactic-co-glycolic acid).